

Article

Enrichment of Coal-Hosted Graphite Deposits Caused by Magmatic Heat Transfer and Tectonic Stress at Feng County, Western Qinling Orogen, China

Yangwei Feng ^{1,2,*} , Yan Ren ¹  and Lushi Lyu ³

¹ Henan Province Engineering Research Center of Environmental Laser Remote Sensing Technology and Application, Nanyang Normal University, Nanyang 473061, China; renyan20202013@126.com

² State Key Laboratory of Continental Dynamics, Northwest University, Xi'an 710069, China

³ Aerophotogrammetrical Surveying and Remote Sensing Bureau, CNACC, Xi'an 710054, China; lyulsarsc@163.com

* Correspondence: 2005130009@163.com

Abstract: China has ranked first worldwide in graphite imports in recent years, facing a graphite supply risk. Coal-hosted graphite is the focus of future graphite deposit exploration. The current research on the enrichment and mineralization mechanism of coal-hosted graphite is superficial, and the identification standard of coal-hosted graphite is incomprehensive, restricting the exploration of coal-hosted graphite mineral resources and the development of coal metamorphic evolution theory. In this study, the Caotangou–Meigou coal-hosted graphite deposit in western Qinling Mountain was taken as a case study for dissection. Based on the data from 1/50,000 and 1/200,000 regional geological mapping and the data of graphite mines in the study area, the samples were systematically collected and analyzed to explore the mechanism of coal graphitization through a 1:5000 geological profile survey, 1/10,000 geological mapping in key areas, and the investigation and cataloguing of abandoned coal-hosted graphite adit. The result was that there were two main coal-hosted graphite ore bodies, striking from nearly east to west. The R_{\max} values of the samples were 7.23–8.15%, the average values of V_{daf} were around 5.0%, the d_{002} value of the II ore body was 0.3433–0.3389 nm, the d_{002} value of the I ore body was mainly 0.3418–0.3429 nm, the graphitization degree G value of the II ore body was 8.14–59.30%, the graphitization degree G value of the I ore body was 12.79–25.58%. The II ore body was coal-hosted graphite, while some samples of the I ore body were coal-hosted graphite, and some samples were coal. The magmatic heat controls the thermal metamorphism of coal seams to form graphite. The closer the distance to the magma body, the larger the crystals, and the higher the euhedral degree, indicating the higher degree of coal seam metamorphism. The nearly north–south compressive structures mainly provided effective tectonic stress for the evolution of coal graphitization during the Yanshan period; the basic structural units (BSUs) rotated and rearranged, eventually forming a straight graphite structure, and tectonic stress catalyzed the graphitization process. The coal-hosted graphite deposits formed under the dual effects of magmatic heat transfer and tectonic stress.

Keywords: coal-hosted graphite; graphitization; magmatic heat; tectonic stress; Qinling orogen



Citation: Feng, Y.; Ren, Y.; Lyu, L. Enrichment of Coal-Hosted Graphite Deposits Caused by Magmatic Heat Transfer and Tectonic Stress at Feng County, Western Qinling Orogen, China. *Minerals* **2023**, *13*, 1258. <https://doi.org/10.3390/min13101258>

Academic Editor: Jan Marten Huizenga

Received: 18 August 2023

Revised: 19 September 2023

Accepted: 25 September 2023

Published: 27 September 2023



Copyright: © 2023 by the authors. Licensee MDPI, Basel, Switzerland. This article is an open access article distributed under the terms and conditions of the Creative Commons Attribution (CC BY) license (<https://creativecommons.org/licenses/by/4.0/>).

1. Introduction

The coal-hosted graphite is a common coal-bearing non-metallic mineral [1,2], which is an emerging strategic mineral resource indispensable for military and modern industrial development [3–5]. Meanwhile, the development and utilization of graphene have elevated the use of graphite to a new level [6,7]. Though the graphite production in China has steadily ranked first worldwide in recent years [8], China must import tens of thousands of tons of graphite each year [9]. Thus, there is a supply risk of graphite, particularly high-quality graphite, in China [4,10].

China is rich in coal-hosted graphite resources [11], which has significant advantages, including high grade, concentrated distribution, large seam thickness, and easy exploitation [12,13], so it is one of the main avenues for graphite exploration in the future [14]. The Qinling orogenic belt is an essential coal-hosted graphite resource distribution area in China [12] and an ideal natural laboratory for studying coal-hosted graphite mineralization. Several coal-hosted graphite deposits have been discovered in Qinling orogen [13,15], and the significant deposits are the Caotangou–Meigou graphite deposit in Feng County of Shaanxi Province in West Qinling orogen [16], and the Yangshan graphite deposit in Shangcheng County [17] and the Dazhuang graphite deposit in Lushan County [18] of Henan Province in East Qinling orogen. Coal-hosted graphite resource prospecting areas have also been discovered at Gangou of Wulichuan Town in Lushi County and Longtangou in Nanzhao County in Henan Province (Figure 1).

Coal is an organic rock that is very sensitive to geologic conditions, such as temperature and pressure [19]. Studies on the graphitization of coal have been previously conducted by scholars worldwide. The earliest research on coal metamorphism and transformation into graphite abroad was based on Hilter's (1873) theory of coal deep metamorphism—Hilter's law. Professor Yang Qi is a representative researcher on coal metamorphism in China [20]. The research work of previous scholars has shown that temperature [21–23], tectonic stress [17,19,24–26], and even chemically active fluid [20,27] are important factors causing coal graphitization. Some scholars even conducted experiments to study the graphitization of coal [28–30]; some other scholars began to focus on graphitization through the evolution of nanostructure of coal-hosted graphite [31–33], but the coal graphitization experiment resulted in relatively poor results. However, the research into the mechanism of coal-hosted graphite mineralization is still insufficient. There is also no standard specification specifically for coal-hosted graphite identification [1], raising a relatively high risk of resource waste. Geological teams [34,35], enterprises [36] and scholars [16,37,38] have conducted surveys on coal-hosted graphite deposits in Feng County, Shaanxi Province, and their work confirmed the existence of coal-hosted graphite in the study area. However, the research on enrichment of coal-hosted graphite is still relatively weak in Feng County, restricting the exploration of coal-hosted graphite resources. Therefore, the mineralization mechanism of coal-hosted graphite needs to be carried out as soon as possible.

The objective of this study is to investigate the enrichment mechanism of coal-hosted graphite under the combined effects of magmatic heat transfer and tectonic stress in Feng County, Western Qinling orogen. For this purpose, the Caotangou to Meigou coal-hosted graphite deposit in Feng County was chosen as a typical case. Based on the data from regional geological surveys, the work of geological mapping, geological profile surveys, cataloguing of abandoned graphite deposits and adits was carried out. Samples were systematically collected at the same time and analyzed in the laboratory later. The corresponding relationships between temperature, pressure, crystal structure, and graphitization degree in the graphitization process of coal needed to be established. The coordination between magmatic heat and tectonic stress was discussed.

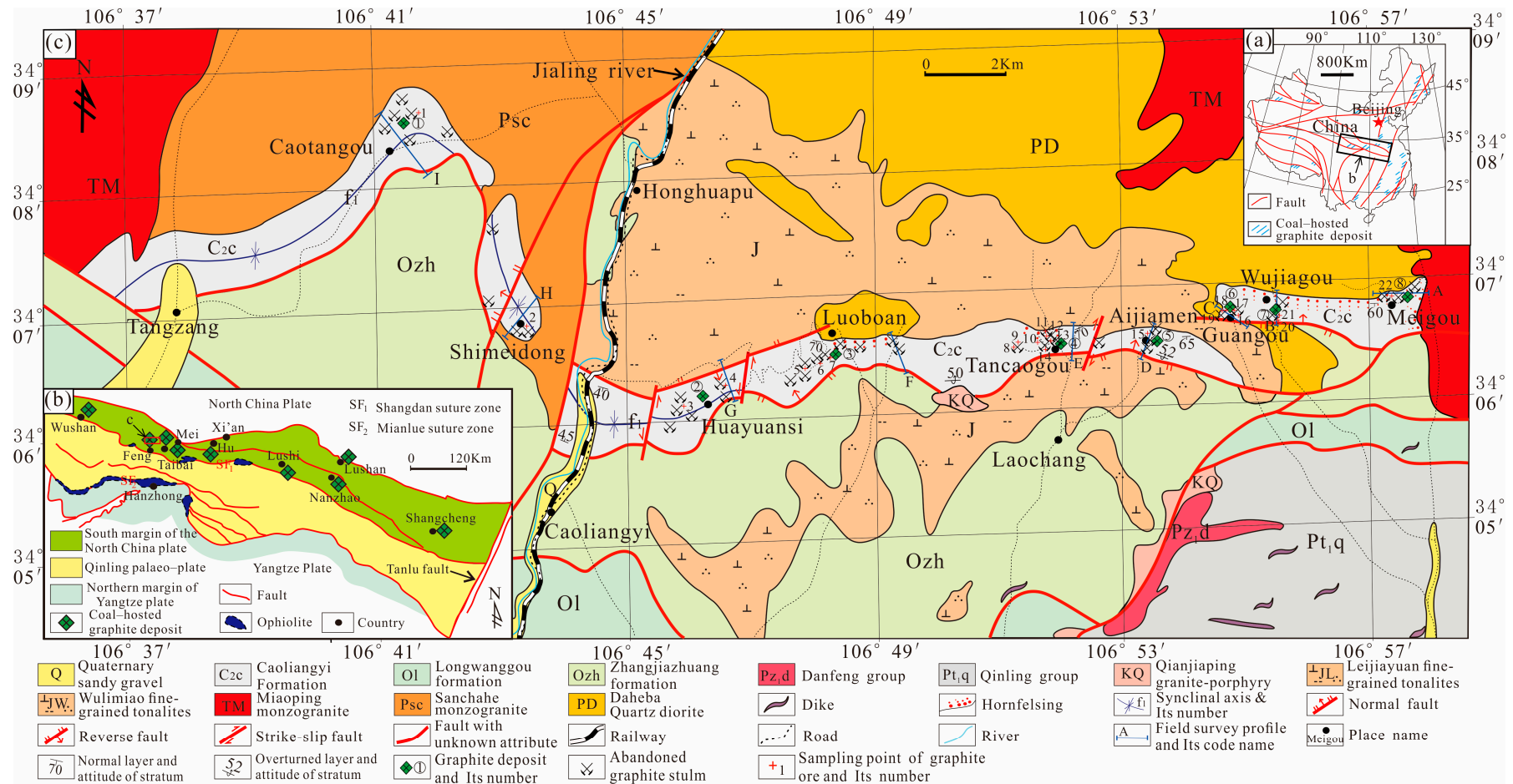


Figure 1. (a) Sketch map of coal-hosted graphite distribution in China [12]. (b) Simplified Structural Map of the Qinling Orogenic Belt [39] and distribution of coal-hosted graphite in Qinling area. (c) Sketch map of geological outline and coal-hosted graphite distribution in Caotangou to Meigou area of Feng County, West Qinling orogenic belt (adapted from [13,34]). Field geological survey profiles: A. Meigou profile; B. Wujiagou profile; C. Guangou profile; D. Aijiamen profile; E. Tancaogou profile; F. Longwanggou profile; G. Huayuansi profile; H. Shimeidong profile; I. Caotangou profile. Key graphite deposit: 1. Caotangou graphite deposit; 2. Zengjiawang graphite deposit; 3. Luoboan graphite deposit; 4. Tancaogou graphite deposit; 5. Xinda graphite deposit; 6. Longtai graphite deposit; 7. Tangjiawan graphite deposit; 8. Huasheng graphite deposit.

2. Geological Setting

2.1. Geotectonic Position

The Qinling orogenic belt is a significant coal-hosted graphite distribution area in China [11,13,39]. The Caotangou to Meigou graphite deposit in Feng County is located at the transition between the Eastern and Western Qinling orogen, in the southern margin of the imbricated thrust nappe tectonic belt of the Northern Qinling Mountains, adjacent to the western Qinling–Songpan tectonic junction in the west, connected to the Baoji rock mass in the north, and adjacent to the Shangdan suture zone of the Qinling orogenic belt in the south [40–42] (Figure 1a,b).

2.2. Exploration and Development History of Mineral Deposits

Different degrees of coalfield geology, graphite deposit and regional geological surveys have been carried out in Feng county area since the 1960s. From 1960s to 1980s, the government of Feng county operated coal mines in Caotangou and Luobaoan in the study area. In 1959, the Hanzhong exploration team of Shaanxi Coal Industry Bureau conducted a coal resource investigation in the Caoliangyi area, and the result showed that the coal is anthracite, and the coal seam is unstable. In 1960, the Qinling Regional Geological Survey Brigade of Shaanxi Provincial Geology Bureau conducted the investigation of coal-hosted graphite from Meigou to Guangou. The investigation revealed that the shapes of graphite ore bodies are stratiform-like and lenticular, the length of ore bodies is about 650 m, and the average thickness of ore layers is 2.2 m, which demonstrated the existence of coal-hosted graphite resources in this area. In June 1983, the No. 185 coalfield geological survey team of Shaanxi Province submitted the geological data of coal in Luobaoan. The coal was found to be a high-metamorphic anthracite, with lenticular shape and labile thicknesses. From 1993 to 1995, a 1/50,000 regional geological survey was conducted in the study area by the regional geological survey brigade of Shaanxi Bureau of Geology and Mineral Resources. From 2013 to 2018, the Bureau of Aerial Survey and Remote Sensing of the General Administration of Coal Geology of China conducted a survey of coal-hosted graphite from Caoliangyi to Laochang. Information regarding ore-bearing strata, ore types, and quality was surveyed, and the graphitization of coal was found, but the study of the graphite mineralization mechanism was insufficient. Wei et al. (2017) discussed the control of tectonism on coal-hosted graphite mineralization in the Caoliangyi to Laochang area [37]. Feng et al. (2018) studied the geological characteristics of coal-hosted graphite deposits from the Caotangou to Meigou area [16]. The Xinda graphite deposit, the Guangou graphite deposit, the Tangjiawan graphite deposit, the Longtai graphite deposit and the Meigou graphite deposit were sequentially shut down by the end of 2020 in the eastern part of the study area. Currently, there are no graphite deposits being mined in the research area.

2.3. Regional Stratigraphy and Tectonics

The strata in the study area are mainly the Proterozoic and Lower Palaeozoic, including the gneisses and marble of the Lower Palaeozoic Qinling Group (Pt_1q), the intermediate basic volcanic mixed with pyroclastic rocks of the Lower Palaeozoic Danfeng Group (Pz_1d), the spilite–quartz keratophyre sequence of the Ordovician Zhangjiazhuang Formation (Ozh), the acidic volcanic sedimentary rocks of the Longwanggou Formation (Ol), and the low-grade metamorphic graphite slate, metamorphic quartz conglomerate, quartzite and metasandstone of the Upper Carboniferous Caoliangyi Formation (C_2c). The intrusive rocks in the study area include the Cretaceous Qianjiaping granite–porphyry (KQ), the Jurassic Leijiayuan fine-grained tonalites (JL) and the Jurassic Wulimiao fine-grained tonalites (JW), the Triassic Miaoping coarse-grained monzogranite (TM), the Permian Sanchahe coarse-grained monzogranite (PSC), and the Permian Daheba coarse-grained quartz diorite (PD). The main occurrence is a batholith.

The area extrudes in the north–south direction, forming the Luobaoan–Aijiamen syncline. The eastern part is the remaining northern limb of the syncline, where the dipping angle is large, and regional areas are nearly upright. The western syncline opens toward the

southwest, and the limb is steep in the north and gentle in the south. Secondary folds developed here, and many small, overturned anticlines and recumbent folds can be observed (Figures 2 and 3).

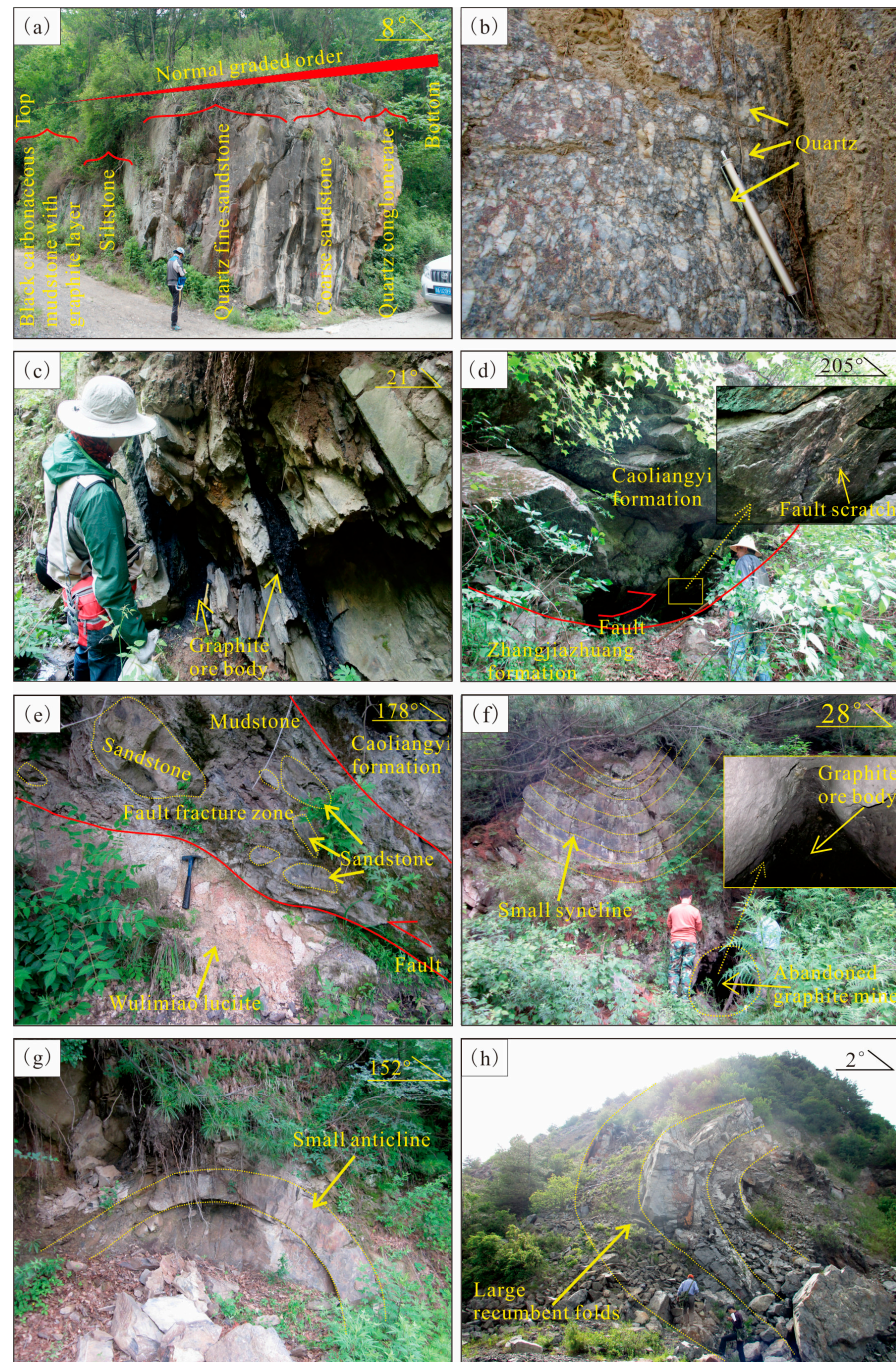


Figure 2. Photos of field outcrops in Caotangou to Meigou graphite deposit, Feng County. (a) Single stratigraphic sequence of Caoliangyi Formation in Tancaogou, the occurrence of the strata is nearly vertical; (b) Metaquartzite conglomerate at the bottom of one single stratigraphic sequence of Caoliangyi Formation in Tancaogou, most quartz particles were flattened and elongated; (c) Graphite ore outcrop at abandoned graphite stupa in Tancaogou; (d) The Caoliangyi Formation thrust over the Zhangjiazhuang Formation in Longwanggou; (e) The Caoliangyi Formation thrust over on the Wulimiao lucite in Huayuansi; (f) The abandoned graphite stupa was located at the core of a syncline in Huayuansi; (g) The small anticline of Caoliangyi Formation in Huayuansi; (h) Large recumbent folds developed in Caoliangyi Formation in Luoboan, metaquartz conglomerate was involved.

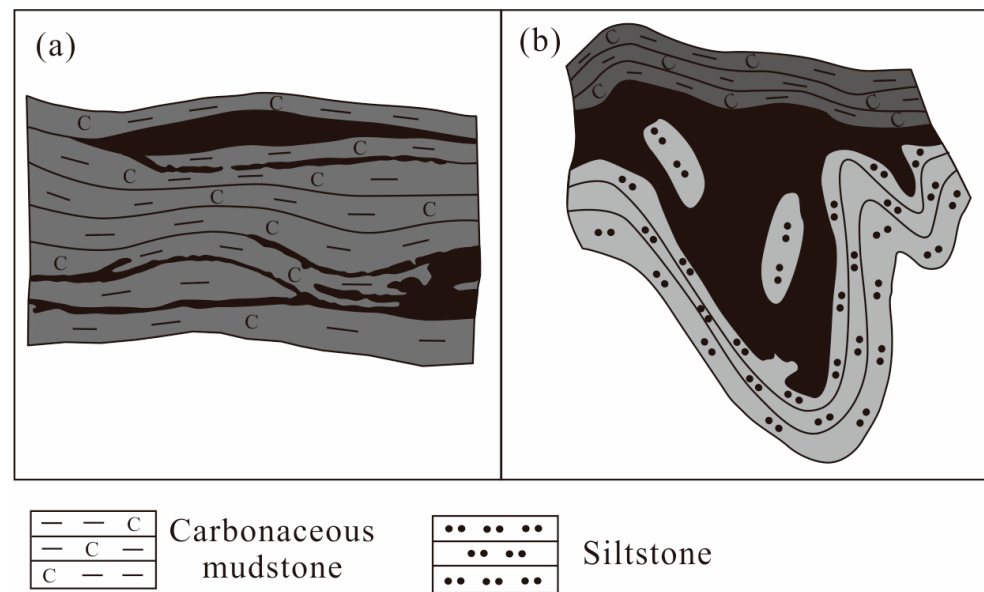


Figure 3. Sketch map of common graphite ore body morphology: (a) branched ore body; (b) lenticular ore body.

2.4. Ore-Bearing Strata

The ore-bearing strata in the study area are from the Upper Carboniferous Caoliangyi Formation (C_{2c}). The strata underwent shallow metamorphism, and the lithology is composed of cinerous–incanus graphite slate, metamorphic quartz conglomerate, quartzite, and metamorphic sandstone. The primary rocks of the Caoliangyi Formation were developed by the fluvial facies and swamp facies coal-bearing clastic, which is multicycle, and developed under a warm and humid climate from the end of the Early to Late Carboniferous. The stratigraphy of the Upper Carboniferous Caoliangyi Formation in the study area exhibits a cyclic structure, which is subdivided into seven small sequences from the bottom to the top based on the characteristics of the thick basal conglomerate and coal bed/black carbonaceous mudstone within each small sequence that can be compared throughout the area. The lower part of the cycle consists of thick layers of massive metamorphic quartz conglomerate with inconspicuous stratification, massive structure, and blastopsephitic texture. The gravel is dominated by quartz and sub-angular or sub-circular composition, the particle size is 1 cm to 3 cm, the content is more than 80% siliceous cement, and the conglomerate stacked tile arrangement can be observed in the regional area. The middle part is quartzite and metamorphic sandstone, which is hard and dense, with palimpsest plane and cross-bedding. The upper part is a deep grey and grey-black shale of carbonaceous slate, and a graphite slate with a palimpsest wavy bedding, a massive structure, and visible plant fossil fragments (Figure 4). The roof and bottom of the ore body of the Caoliangyi Formation in the study area are embroiled in the interior of the ore body due to fault dislocation, rock encroachment, and tectonic uplift denudation during the late deposition period. The eastern part of the strata is the remaining northern limb of the syncline, which steeply dips to the south. Most of the dip angles of the strata are between 60 and 80 degrees. The syncline at the western part is nearly intact, opening to the southwest, and is steep on the north limb and gentle on the south limb. The western and eastern parts of the southern flank connect the Ordovician Caotangou Group metavolcanic clastic rocks, and the middle part connects to the Yanshanian Leijiayuan fine-grained diorite by the low-angle thrust fault. Regional areas were reformed by the Cretaceous Qianjiaping granite porphyry. The northern strata were intruded by the coarse-grained monzogranite, coarse-grained quartz diorite, and Yanshanian fine-grained tonalite (Figure 2).



Figure 4. Photos of coal-hosted graphite ore in Caotangou to Meigouarea, Feng County. (a) Graphite ore in Guangou graphite deposit; (b) Graphite ore in Wujiagou graphite deposit; (c) Graphite ore in Tancaogou graphite deposit; (d) Graphite ore in Caotangou graphite deposit; the fossil plant is visible. Gph: graphite; And: andalusite.

3. Data and Methods

3.1. Samples

The study included a literature review, field geological surveys, sample testing and analysis, and comprehensive indoor investigations. First, data, such as the basic geological reports, mineral geological reports, and scientific and technical papers of the study area, were collected to identify the scientific problems. Based on the research results of the 1/50,000 regional geological survey of the Honghuapu and Xinjiazhuang and the 1/200,000 regional geological survey of Xiangquan, nine 1/5000 field geological survey routes were formulated in detail, with a total length of 13.98 km. In the area of Caoliangyi to Laochang, a key coal-hosted graphite deposit in Feng County, West Qinling, 1/10,000 basic geological mapping was conducted, covering an area of approximately 15 km². Five boreholes were catalogued, 23 flat tunnels of old graphite mines were observed and catalogued, more than 1000 photos were taken, and more than 200 rock samples were collected, including 106 thin sections samples, 30 probe slices samples, 12 SEM (scanning electron microscope) samples, 10 XRD (X-ray diffraction) samples, and 22 graphite ore samples (Table 1).

Table 1. List of geological survey workloads for the research projects.

Order Number	Geological Profile			Number of Samples				Graphite Ore	The Figures Belong
	Number	Name	Length/km	Thin Section	Probe Slices	SEM	XRD		
1	A	Meigou	1.15	12	6	2		1	Figure 5b;
2	B	Wujiagou	1.00	2	1	1	2	2	Figures 4b and 5d;
3	C	Guangou	0.90	9	1	3	3	4	Figures 4a and 5a;
4	D	Aijiamen	0.95			1	1	1	
5	E	Tancaogou	2.60	54	10	1		7	Figures 2a–c, 4c, 5c, 6c,d and 7b,f–h;
6	F	Longwanggou	1.20	17	5			3	Figures 2d,h, 6a,b and 7c,d;
7	G	Huayuansi	0.88	3	2			2	Figure 2e–g;
8	H	Shimeidong	3.20	5	1	1	2	1	Figure 7a,e;
9	I	caotangou	2.10	4	4	3	2	1	Figure 4d;
	Total		13.98	106	30	12	10	22	

3.2. Experimental Testing

The work of thin sections and probe slice grinding was carried out in the laboratory of the regional geological and mineral research institute of the Shaanxi provincial bureau of geology and mineral exploration and development. Thin section identification, probe slices analysis, SEM observation, and X-ray diffraction (XRD) analysis were conducted at

the Northwest mineral resources supervision and testing centre, the Ministry of Natural Resources of China. The instrument used for thin section identification was a Leica polarizing microscope, the main content of identification was a rock structure with texture and mineral identification. The model of the instrument used for probe analysis was JXA-8530F Plus, of which the main attachment was the Oxford X-Max20 energy spectrometer. Through quantitative analysis of the micro-zone composition of a single mineral, the characteristic metamorphic minerals were identified by probe analysis. The instrument used for SEM was JSM-7500F made in Japan, equipped with an X-Max 50 X-ray spectrometer from Oxford, UK. The working voltage of JSM-7500F was 15 kV, the spectral resolution was better than 127 eV (Mn K α , the counting rate is 20,000 cps). Scanning microscope analysis observed the microscopic morphology of the sample, including crystal size and degree of automorphism. The model of the X-ray diffractometer was D/MAX-2500, of which the main test conditions were the Cu target, the working voltage was 40 kV, the working current was 40 mA; continuous scanning was also performed. X-ray diffraction analysis was used to determine the crystal structure and graphitization degree of the sample through the pattern. The test of graphite ore was carried out at Key Laboratory of Coal Resources Exploration and Comprehensive Utilization, Ministry of Natural Resources, China. The important test items of graphite ores are mainly fixed carbon content, vitrinite reflectance (R_o), apparent density, moisture content, ash content, volatile matter, etc. The determination of fixed carbon content adopts the indirect carbon determination method. After measuring the volatile and ash content of the sample, their values were subtracted from the total amount, and the difference as the fixed carbon content. The executive Standard is GB/T3519-2008 [43] Amorphous graphite.

3.3. Research Method

In this project, a field geological survey was conducted in representative areas of coal graphitization in Feng County, western Qinling orogenic belt. The key investigation objects were the ore bearing construction of the Caoliangyi Formation, its thermal contact metamorphic zone contacting with igneous rock intrusion, and the structural deformation area. Two types of profiles were selected in field geological survey: the first type of profile is the thermal contact metamorphic zone with strong magmatic thermal contact metamorphism and weak tectonic stress background, and the second type of profile is a geological profile with varying degrees of structural deformation (strong, relatively strong, weak) and weakly affected by magmatic heat. The direction of the profile is perpendicular to the direction of the strata or the main structural line. The phenomena of mineralization and alteration, stratigraphic lithology, contact relationships, and structural deformation characteristics were described. The development of rock keratinization, hydrothermal quartz veins, and conjugated shear joints were paid attention to. The graphite ore samples were collected using the grooving method; each sample was approximately 3–5 kg. All rock samples needed to be accurately and accurately marked with their positions on the profile, and a rock sample size of 3 cm \times 6 cm \times 9 cm was appropriate. In the field, geological phenomena were recorded in detail, photographs were taken, and relevant rock samples were collected.

The samples testing and analysis were conducted indoors. The petrology and petrography characteristics of rocks in thermal contact metamorphic zone were observed, which helped to identify the characteristic metamorphic minerals with temperature and pressure indications and determine the degree of thermal contact metamorphism. Mainly based on the occurrence statistics of conjugate shear joints, assisted by analysis of small faults and folds, combined with the microstructure of deformed rocks, the ancient tectonic stress field was restored. Based on the testing of graphite ore samples, the characteristics, such as the fixed carbon content, crystalline size, and the euhedral degree of the graphite, were determined by analyzing the graphite ore samples in the plane and longitudinal directions. Through comprehensive analysis, detailed discussions were conducted on the types and degrees of thermal conditions and spatial locations of the magmatic intrusions that potentially

affected coal metamorphism and graphite formation. The superposition effect of magmatic intrusions of different ages was also analyzed. The influence of different-strength structural stresses on coal graphitization degree, graphite crystal structure parameters, and other characteristics was discussed. The mechanism of coordinated action between magmatic heat and tectonic stress during the graphitization process of coal seams was explored.

4. Results

4.1. Ore Body Characteristics

There are several coal-hosted graphite ore bodies developed in the Caotangou to Meigou graphite deposit area. Due to magma intrusion, fault damage, and ore bed branching and pinching out, the graphite ore bodies are of poor continuity. Through comparative analysis of rock layers and ore-bearing layers, it was determined that there are two main graphite ore bodies, named No. I and No. II (Figure 1). The No. I graphite ore body is located in the cinerous–incanus graphite slate, striking nearly from east to west. The No. I ore body is composed of four branch ore layers; the strike lengths of one single ore layer were about 1400 m, 6200 m, 2430 m, 1400 m, and the corresponding seam thicknesses of the No. I ore body were 1.00–4.00 m (average 2.10 m), 0.65–1.44 m (average 0.93 m), 0.30–2.90 m (average 1.20 m), and 0.35–6.50 m (average 1.95 m). The No. II graphite ore body is located in the cinerous–incanus graphite slate, striking nearly from east to west. The No. II ore body is composed of three branch ore layers; the bifurcation of the ore body was randomly visible. The strike lengths of one single ore layer were about 2100 m, 1100 m and 2500 m, and the corresponding seam thicknesses of the No. II ore body were 0.15–3.80 m (average 1.52 m), 0.45–5.52 m (average 2.33 m), and 0.15–6.80 m (average 2.45 m).

Under the control of syncline tectonics and stratigraphic occurrence, the morphology of the ore body showed the main northern limb of the syncline, which steeply dips to the south. Most of the dip angles are between 60 and 80 degrees. The western part is a near-complete syncline, with the opening facing southwest; the north limb is steep, and the south limb is gentle. The individual ore bodies are lenticular, branched and stratiform-like (Figure 3). The regional ore bodies are thickened by tectonic compression with a single enclave and multiple enclaves intermittently connect in a podiform.

4.2. Ore Characteristics

The graphite ore in the study area is aphanitic graphite, the macroscopic state is similar to that of soil, and the color is gray black, steel gray. The ore is soft with low hardness and uneven fracture morphology. It is slippery-feeling with the ability to easily stain hands. There is metallic to submetallic luster, and the friction mirror surface is visible at the surface of graphite ores. The coal-hosted graphite ore body is lenticular and stratiform-like, with flaky structure and xenomorphic lepidoblastic texture (Figure 4).

4.3. Ore Composition

Based on rock thin section identification and electron probe analysis, it was determined that the ore is dominated by graphite, quartz, and a small amount of andalusite, sillimanite, clay minerals, pyrite, and trace limonite. The mineral composition is mainly fixed carbon, and the content is mostly 63.52% to 87.77%.

The I ore body: The fixed carbon content is 54.00–70.09%, with an average of 63.52%. The ash content is between 18.2 and 40.10%, with an average of 31.13%. The total sulfur content is 0.06–0.46%, with an average of 0.31%. The volatile matter (V_{daf}) is 4.12–4.9%, and the average is 5.18%. The apparent density is between 1.66 and 2.13 g/cm³, and the mean is 1.96 g/cm³. The vitrinite reflectance R_{max} is 7.37–7.71%, with an average of 7.45%.

The II ore body: The fixed carbon content is 69.21–90.05%, with an average of 83.98%. The ash content is 5.69–28.07%, with an average of 12.00%. The total sulfur content is 0.06–0.66%, with an average of 0.23%. The volatile matter (V_{daf}) is 2.72–5.63%, with an average of 3.93%. The apparent density is 1.73–2.14 g/cm³, with an average of 1.87 g/cm³, and the vitrinite reflectance R_{max} is 7.23–8.15%, with an average of 7.51% (Table 2).

Table 2. Test data of coal-hosted graphite ore samples from Caotangou to Meigou in Feng County.

Sample Number	Sample Point		Ash Content A _d /%	Volatile Matter V _{daf} /%	Total Sulfur S _{td} /%	Fixed Carbon FC _d /%	Apparent Density /g·cm ⁻³	Average Maximum Vitrinite Reflectance R _{max} /%	Interplanar Spacing d ₀₀₂ /nm	Graphitization Degree G/%	Ore Body Number
	Longitude	Latitude									
1	106°41'31.53"	34°8'28.86"	39.58	6.42	0.33	54.00	1.98	7.11	0.3622	-	I ore body
2	106°43'15.33"	34°6'49.47"	36.11	4.32	0.47	59.57	2.05				
3	106°46'09.22"	34°6'05.36"	39.34	5.35	0.27	57.41	1.66	-			
4	106°46'49.52"	34°6'26.32"	27.88	5.47	0.46	66.87	1.98	7.71	0.3418	25.58	
5	106°47'38.84"	34°6'27.60"	24.01	4.12	0.25	69.96	1.95	7.43	0.3426	16.28	
8	106°51'19.20"	34°6'35.26"	18.22	5.53	0.26	75.29	1.87	7.65	0.3429	12.79	
9	106°51'20.36"	34°6'35.42"	23.76	5.34	0.06	70.09	2.13	7.37			
15	106°53'46.07"	34°6'31.77"	40.10	4.90	0.37	55.00	2.02				
	average		31.13	5.18	0.31	63.52	1.96	7.45	0.3428	18.22	
6	106°47'53.36"	34°6'29.12"	9.56	4.43	0.24	84.71	1.81	8.15	0.3389	59.30	II ore body
7	106°48'2.32"	34°6'30.07"	17.24	4.28	0.43	76.23	1.90	7.50			
10	106°51'41.32"	34°6'31.33"	28.07	2.72	0.06	69.21	1.99	7.28	0.3433	8.14	
11	106°51'49.14"	34°6'41.43"	18.53	5.63	0.18	76.88	1.79	-			
12	106°51'49.17"	34°6'41.33"	10.78	5.05	0.25	84.71	1.82	-			
13	106°51'49.24"	34°6'41.28"	7.87	3.07	0.08	89.31	2.01	7.23	0.3421	22.09	
14	106°51'49.15"	34°6'31.35"	13.06	3.92	0.08	83.53	1.98	-			
16	106°55'1.58"	34°6'27.06"	6.37	4.63	0.08	89.00	1.75				
17	106°55'23.96"	34°6'38.29"	8.44	3.18	0.11	88.38	1.78	7.32	0.3419	26.25	
18	106°54'32.20"	34°6'43.53"	9.91	3.89	0.66	86.20	1.80				
19	106°54'31.85"	34°6'42.33"	11.42	3.68	0.18	84.90	1.85	7.42			
20	106°56'47.64"	34°6'18.63"	5.69	4.26	0.49	90.05	1.73				
21	106°56'39.95"	34°6'25.37"	12.10	3.03	0.16	84.87	1.88	7.58	0.3406	39.53	
22	106°57'21.37"	34°6'50.42"	8.96	3.27	0.15	87.77	2.14	7.39	0.3392	55.81	
	average		12.00	3.93	0.23	83.98	1.87	7.51	0.3410	35.19	

Note: $G = (0.3440 \text{ nm} - d_{002}) / (0.3440 - 0.3354 \text{ nm})$; The sampling point location is shown in Figure 1.

According to the research results of professor Cao Daiyong's team regarding the identification standard of coal-measure graphite, the preliminary identification indexes of coal-measure graphite are obtained, including the volatile $V_{daf} < 5.0\%$ and the maximum reflectivity $R_{max} > 6.0\%$ [3,14]. The R_{max} values of the samples in Feng County are all greater than 6.0%. The V_{daf} values of the samples from the II ore body are all less than 5.0%. The V_{daf} values of the samples from No. I ore body are around 5.0%. All fixed carbon content values are greater than 55%, meeting the requirements for the fixed carbon content of aphanitic graphite. Therefore, it is preliminarily determined that these samples are coal-hosted graphite.

4.4. Graphite Crystal Size and Euhedral Degree

The graphite crystalline form of the Caotangou–Meigou graphite deposit in Feng County is close to hexagonal, with a primarily medium to high euhedral degree; it is fine, scale-like. Graphite of Sample 19 in Guangou is most close to the magmatic intrusion, and the crystalline graphite is close to regular hexagonal and euhedral well-formed sample with a crystal size of $1.5 \mu\text{m} \times 1.3 \mu\text{m}$. Graphite of Sample 22 in Meigou is very close to the Permian magmatic pluton and is euhedral and well-formed, showing a hexagonal shape and straight edges. Several graphite crystals have a low euhedral degree with a crystal size of $0.4 \mu\text{m} \times 0.8 \mu\text{m}$, while several individual crystal sizes can reach $0.85 \mu\text{m} \times 1.1 \mu\text{m}$. Graphite of Sample 9 at the outcrop of Tancogou is relatively less automorphic, with a small proportion of intact crystals and hexagonal shapes. However, the edges are not straight and relatively rough. The larger crystal size is $0.6 \mu\text{m} \times 1.08 \mu\text{m}$. Graphite of Sample 20 at the Wujiagou graphite deposit is fine and dense scale-like, with few hexagonal shapes and poor euhedral degree (Figure 5).

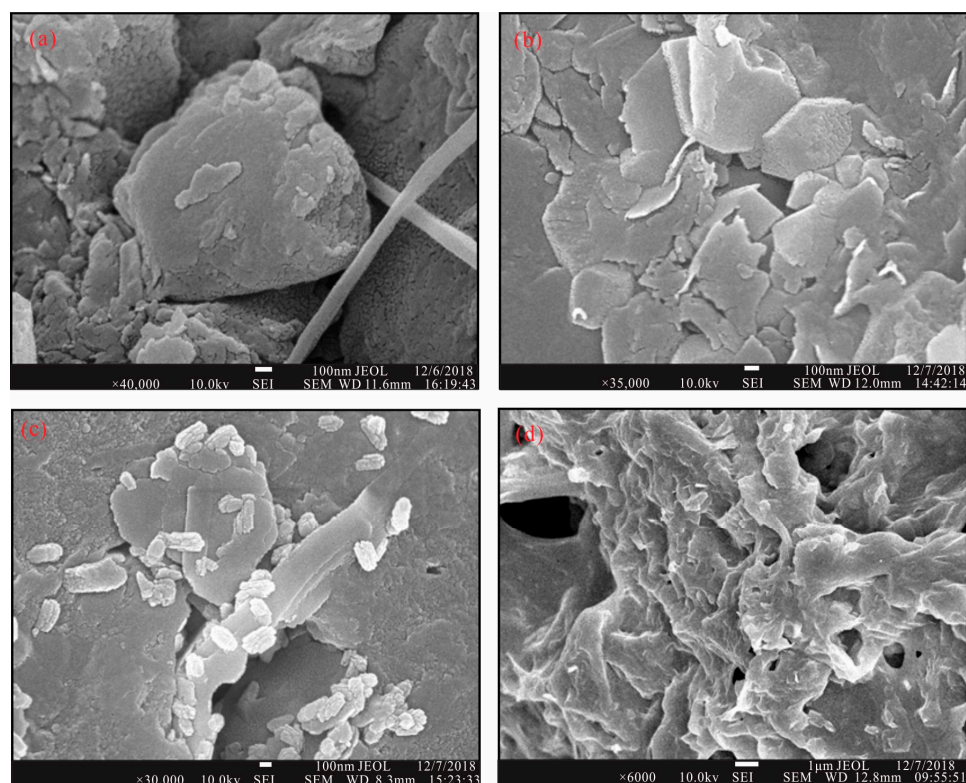


Figure 5. Microscopic characteristics of coal-hosted graphite crystals under scanning electron microscopy in Caotangou to Meigou area, Feng County. (a) Graphite ore in Guangou, Sample 19, euhedral crystal, hexagonal plate-like shape; (b) graphite ore in Meigou, Sample 22, euhedral crystal, hexagonal plate-like shape; (c) graphite ore at outcrop of Tancogou, Sample 9, subhedral crystal, partly hexagonal plate-like shape; (d) graphite ore in Wujiagou, Sample 20, anhedral crystal, stacked shape.

4.5. Graphitization Characteristics

The process of coal graphitization is that in which the original structural defects continuously shrink and eventually disappear [44]. Based on the statistical analysis of the test data, Kwiecińska and Petersen (2004) [45], Rantisch et al. (2016) [46], Lan et al. (2019) [47], Cao et al. (2021, 2022) [3,14], Li et al. (2022) [48], and Wang et al. (2023) [49] scientifically selected identification indexes of coal and coal-hosted graphite, which can be distinguished by interplanar spacing d_{002} and graphitization degree G . The identification indexes of coal-hosted graphite are $d_{002} < 0.3440$ nm, $G > 0$ [3], and the coal-hosted graphite is divided into semi-graphite and graphite [14]. According to the data from Table 2, the d_{002} value of the II ore body is 0.3433–0.3389 nm, with an average of 0.3410 nm; the G value of the II ore body is 8.14–59.30%, with an average of 35.19%. Combining previous R_{\max} and V_{daf} data, it can be determined that the samples of the II ore body consist of coal-hosted graphite. The d_{002} value of the I ore body is 0.3418–0.3429 nm, with an outlier of 0.3622 nm; the G value of the I ore body is 12.79–25.58%, with an average of 18.22%. Combining previous R_{\max} and V_{daf} data, it can be determined that some samples of the I ore body are coal-hosted graphite, and some samples are coal. Meanwhile, the Raman spectroscopy is highly sensitive to the integrity of graphite lattice; the generation of the D 'peak represents the formation of graphite [46,50]. The sample testing results indicate that samples developed D 'peaks in the Caotangou to Meigou graphite deposit, which indicates that the coal seams underwent graphitization in the study area.

5. Discussion

The dual action of magmatic heat and tectonic stress controls the graphitization and mineralization of coal seams. The magmatic thermal emplacement provides sufficient thermodynamic conditions for graphite formation. Moreover, regional metamorphism plays an active role in graphite seam enrichment. The tectonic stress catalyzes the graphitization process and controls the spatial distribution of graphite beds. The core of the secondary anticlines and synclines within the complex fold system is rich in banded enriched graphite deposits.

5.1. Multi-Stage Magmatic Thermal Emplacement in the Qinling Orogenic Belt Provided Sufficient Thermodynamic Conditions for Coal Seam Heating to Form Graphite

The thermal effects of residual magma, magma hydrothermal, and metamorphic heat of the contained radioactive elements increased the ground temperature in the region, forming a geothermal anomaly zone [20]. The main rocks are tonalite, granite and Quartz diorite, which are acidic or moderately acidic, and the acidic magma is highly mobile and conducive to heat transfer. Under thermal contact metamorphism, the organic carbon in coals forms graphite, i.e., the tectonic ordering of carbon. In zeolite-bearing rocks, the organic carbon is still amorphous or only exhibits a partially developed graphite structure. When the rock reaches the epidote amphibolite facies or amphibolite facies, the organic carbon exhibits an ordered graphite structure. In the thermal contact metamorphic zone between the Caoliangyi Formation with the magmatic intrusions in the eastern part of the Caotangou to Meigou graphite deposit in Feng County, the hornfelsification phenomenon indicating thermal contact metamorphism is clearly visible. Flesh-red garnet, an indicator mineral of feldspar–quartz hornstone mineralization, is visible to the naked eye in the contact zone between the rocks in the Longwanggou area and Caoliangyi Formation.

Electron probe experiments on hornfels in the thermal contact metamorphic zone revealed a large number of minerals and assemblages representing thermal contact metamorphism, such as andalusite, chloritoid, chlorite, biotite, and garnet. The rocks exhibited hornfels, porphyritic metamorphic, and massive structure (Figures 6 and 7a,b). The information obtained through the borehole approximately 400 m underground revealed that the rock recrystallization phenomenon is significant, and the black-grey quartz sandstone and quartz conglomerate were practically transformed into grey-white quartzite. The general geological data showed that the graphite distribution zone of the Lutang graphite deposit

in Hunan Province nearly overlaps with andalusite development [12,26]. The distribution of graphite deposits in the study area is closely related to the andalusite and is located at a certain distance from the rock body. The preliminary study indicated that the coal series underwent contact metamorphism by magmatic thermal emplacement with a hierarchical nature. The first stage is rock emplacement, in which tourmalinization, grainization, and alkali metasomatism occur on one side of the rock. Regional melting and migration of boron, fluorine, potassium, sodium, and silicon occur on the contacted side, producing silicification and tourmalinization. This process occurs during magma decompression and volatile consumption. In the second stage, the rocks release heat and heat the surrounding rocks of the coal series, inducing the transformation of the argillaceous content to andalusite or cordierite. After the structural ordering of carbon, the coal seam forms aphanitic graphite.

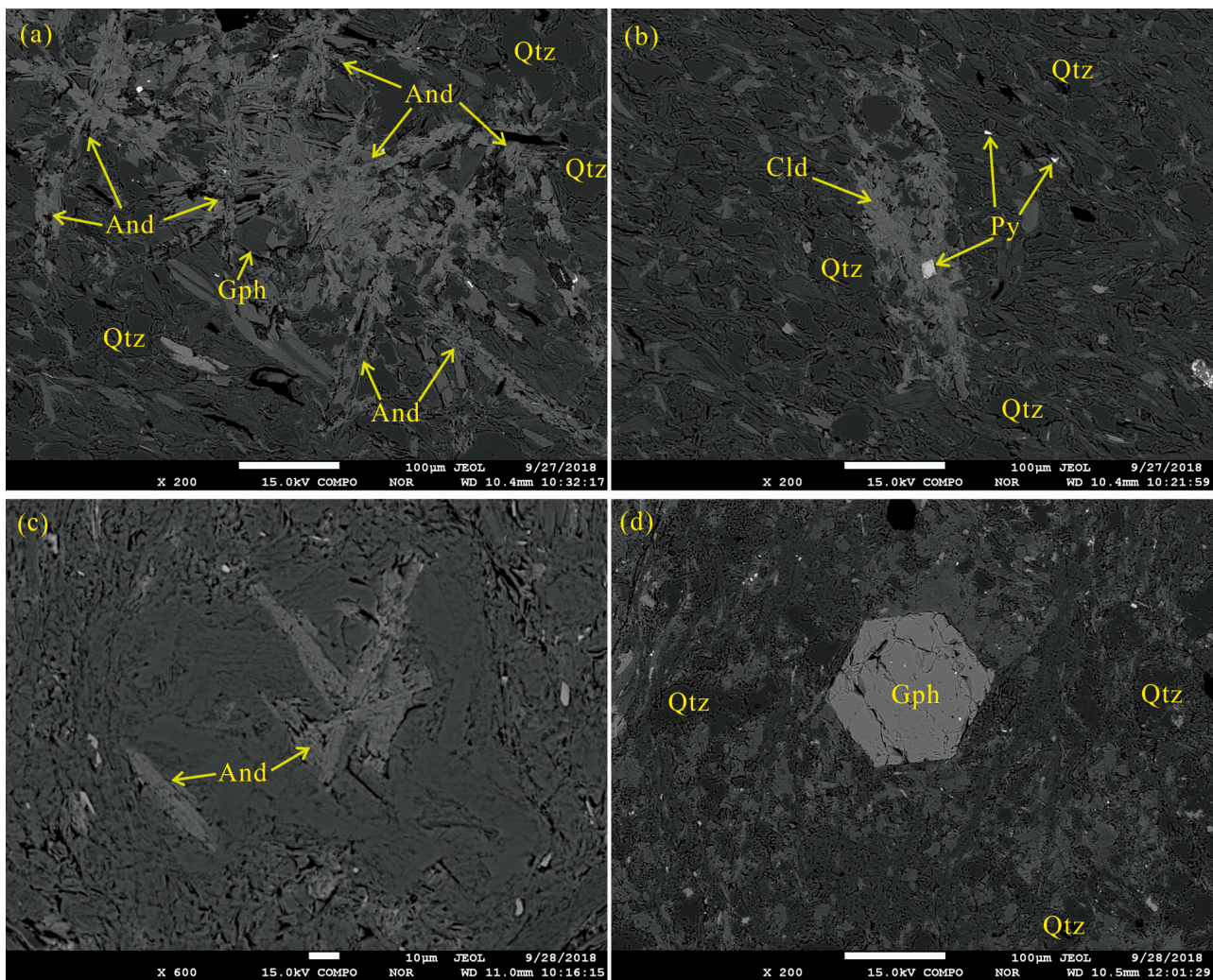


Figure 6. Electron probe photos of Caotangou to Meigou graphite deposit in Feng County. (a) Blake hornfels at Luoboan, andalusite developed with many heteromorphic quartzes; (b) Blake argillite at Luoboan, Chloritoid is visible; (c) black carbonaceous slate at Laochang, andalusite developed; (d) Cataclasite at Tancaogou, hexagonal plate-like graphite is visible, large amount of heteromorphic quartzes developed. Cld: Chloritoid; And: Andalusite; Py: Pyrite; Gph: graphite; Qtz: Quartz.

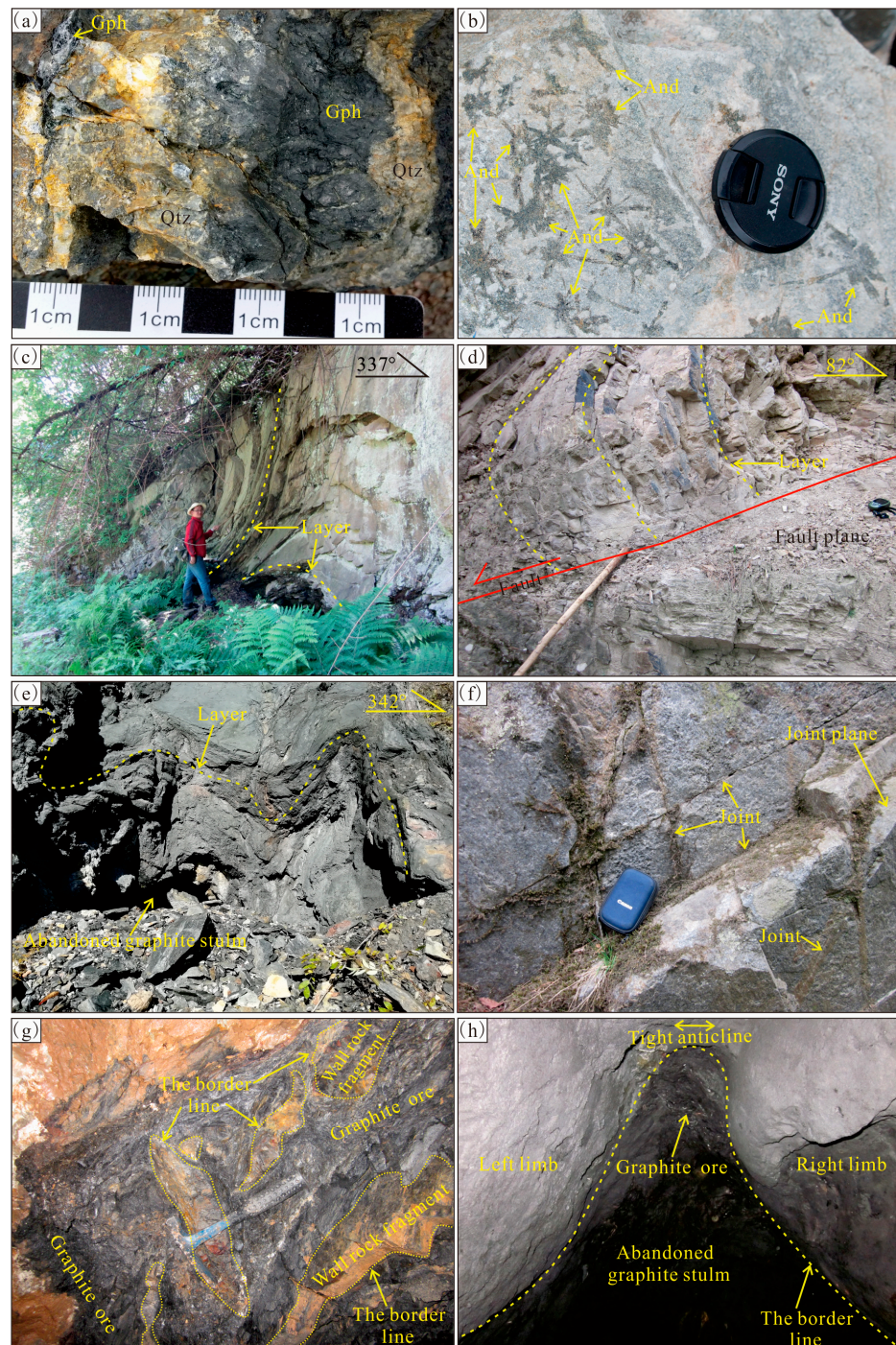


Figure 7. Photos of geological phenomena in the field of Caotangou to Meigou graphite deposits, Feng County. (a) The thermal contact Metamorphic zone at Shimeidong, coal-based graphite is visible; (b) the andalusite hornfels in the north of Tancaogou, andalusite developed; (c) the saddle-shaped structure in Longwanggou; (d) reverse fault in Caoliangyi formation at Longwanggou; (e) the wrinkling phenomenon inside the Caoliangyi Formation at Shimeidong; (f) the joints developed in Leijiyuanlucite in the south of Tancaogou; (g) The graphite in abandoned stulm at Tancaogou, the wall rock was broken; (h) the tight anticline controlled the enrichment position of coal-based graphite in Tancaogou, the abandoned graphite stulm is visible. And: andalusite.

From Figures 1 and 5, it can be seen that the magmatic heat controls the thermal metamorphism of coal seams to form graphite. From Figure 5a (Sample 19), Figure 5b (Sample 22), Figure 5c (Sample 9), and Figure 5d (Sample 20), it can be found that the closer

the distance to the magma body, the larger the crystals, and the higher the euhedral degree, the higher the degree of coal seam metamorphism. The alteration and hydrothermal veins can be commonly found in high-grade metamorphic coal series, and the development of hydrothermal quartz deposits in the surrounding rocks is an important sign of magmatic thermal metamorphism [20]. The development of quartz veins often indicates the intrusion of magmatic rocks [18]. During the magmatic–hydrothermal intrusion, carbon in the enclosing rocks is assimilated by magmatic–hydrothermal fluid, resulting in a significant increase in CO₂ content until the enclosing rocks cool and promote CO₂ reduction in and precipitation of carbon while crystallizing to form graphite. Hydrothermal quartz veins developed in coal-hosted graphite deposits, such as the Caoliangyi, Laochang, Caotangou area in Feng County, Shaanxi Province. Under hydrothermal conditions, the quartz exhibits poor crystal morphology due to lower temperature. In addition, electron probe experiments revealed widespread chloritization alteration in the samples.

5.2. Tectonic Stress Catalyzed the Graphitisation Process

The research area was located in a zone of the Qinling orogenic belt, where the latitudinal tectonic systems are combined with meridional tectonic systems, influenced by the tectonic stresses of the Variscan orogeny [51], Indosinian movement, Yanshanian movement, and Himalayan movement. The Mesozoic magma was frequently and strongly active, particularly in Yanshanian [39]. Based on the 1/5000 geological profile survey and the 1/10,000 geological mapping, the saddle-shaped structures were found developed in the Caotangou to Meigou area of Feng County, which are the results of the superposition of nearly east–west trending folds with northeast or north–south trending folds (Figure 7c,d). Two sets of folds intersect and overlap at large angles or right angles. The statistical results of joint occurrence in the research area show that two sets of X conjugate shear joints developed in the area. The dominant orientation of the first set of joints is NNW and NNE directions, and the dominant orientation of the other set of joints is NWW and near-EW. The joints that strike near north to south are cut off and staggered by joints that strike near east to west, which shows that the development of joints striking near the north to south direction was earlier than that of those that strike near the east to west direction (Figure 7f). The research shows that the nearly north–south tectonic compressive stress and nearly east–west tectonic compressive stress developed in the area, and the former developed earlier than the latter.

During the Variscan to Indosinian period, there was a stress background dominated by the north–south compression in Qinling region. The Caoliangyi Formation began to extrude and fold to form anticline f_1 in the study area. In the Late Yanshanian period, the north–south extrusion was again dominant, producing a southward thrust fault system with a near-east–west orientation. The thrust fault system was thrust southward over the Ordovician and Jurassic diorite rocks, producing a series of complex syncline fold systems with a near-east-to-west orientation on the limbs of the syncline due to tectonic extrusion from north to south. Because of the remote effect of the Pacific plate subducting from the east and the Indian Ocean plate subducting from the southwest to the Eurasian plate, the region experienced a nearly east–west compression during the Himalayan period [52]. A series of sinistral strike-slip faults were developed in Caoliangyi Formation, and the north–south structures of this stage were superimposed on the east–west structures of the Variscan–Indosinian–Yanshanian stage.

Under the action of tectonic compressive stress, the deformation of rock layers was concentrated in the non-uniformity of the Caoliangyi formation stratum, which produced many faults and folds, and the small internal fractures and folds were well-developed. The thick sandstone formed large-scale and gentle folds, while the thin layer slate, clay rock, and ore layers formed small-scale and strongly curved tightly closed folds. The structural deformation of coal-hosted graphite in Caoliangyi Formation was very strong, the ore body was hardly broken, and the structure was loose, and friction mirror surface and scale structure are commonly visible.

Most of the graphite-bearing seams in the Caoliangyi Formation were steeply dipping. Owing to the soft and easily deformable nature of seams and the good lubricating effect of natural graphite, the coal-hosted graphite seam was clearly out of coordination with the upper and lower direct roof strata. The graphite seams were strongly modified and often accompanied by faults at the stress release, squeezing into various detachment cavities or structural weak surfaces in a plastic state. The seams appeared lenticular, nest-like, or pod-like in space and were primarily enriched in the nuclei of the secondary anticlines and synclines in the complex fold system.

5.3. Coupling of Tectonic Stress and Magmatic Thermal Processes Controls the Enrichment and Mineralization of Coal-Based Graphite

According to this study, the coupling of tectonic strain energy and magmatic thermal energy is the main controlling factor of coal graphitization. The magmatic activity in the middle stage of the Yanshan Movement provided a strong heat source for coal thermal metamorphism and graphitization. The nappe structure, the gliding nappe structure and the magma emplacement compressive stress in the same period brought about strain energy, which greatly supplemented the activation energy required for long-term ordered rank physicochemical of basic structural units (BSUs) in coal. The stacking effect of BSUs is the microscopic mechanism of coal graphitization. During the evolution of coal graphitization, the directionality of BSUs gradually increased in Caoliangyi Formation. The isolated BSUs evolved from loosed with berry-shaped BSUs to striped patches, eventually forming a straight graphite structure.

During the thermal contact graphitization process, the coal seams in Caoliangyi Formation underwent strong compression and multi-stage magma stamping. Coal is susceptible to pressure effects. Under the catalytic effect of tectonic stress, the graphitization of anthracite increased and formed a scale-like structure, and the spacing between carbon layers gradually decreased. Microscope observations revealed that the magma affected the metamorphism of coal, inducing condensation. A fine-grained structure began to form in the coal seam, and wavy compression crystals with directional arrangement appeared. Under tectonic shear stress, the basic structural units (BSUs) rotated, shifted, and preferentially orientated; the ordered domain increased. The d_{002} spacing gradually decreased, and the La (the lattice constant of the a-axis of crystals) and Lc (the lattice constant of the c-axis of crystals) increased significantly, forming graphitic carbon layers with an ordered structure. The degree of graphitization of coal away from fault and magmatic rock mass was only semi-graphitic and graphitic anthracite. The ore layers are often associated with faults because they are strongly modified as stress release points, and the graphite layers are strongly thickened and enriched in the nuclei of the secondary anticlines and synclines in the complex fold system due to the stress action (Figure 8e,h and Figure 8).

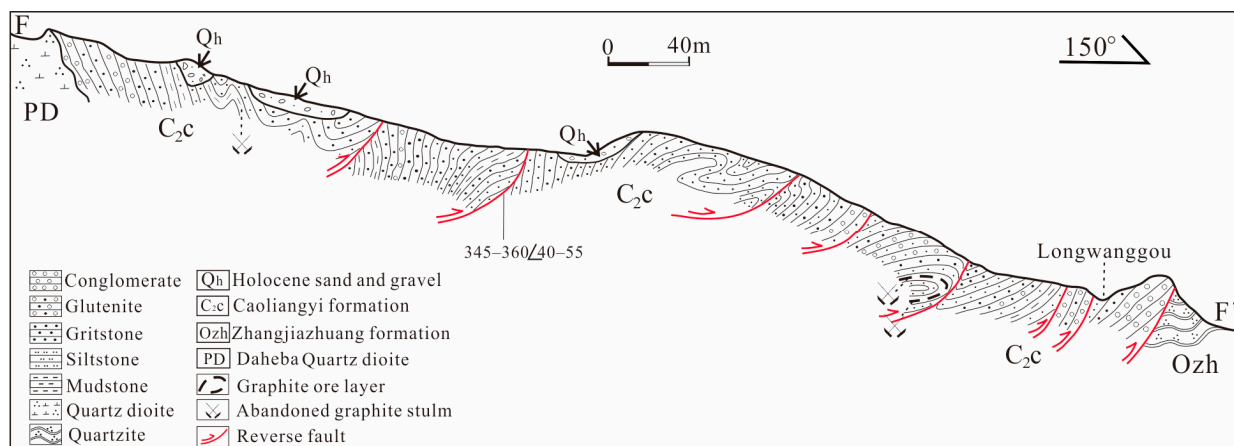


Figure 8. Tectonic geological profile in Longwanggou, Feng County (revised from [13,16,37]).

6. Conclusions

- (1) There are two main coal-hosted graphite ore bodies, striking from nearly east to west. The R_{\max} values of the samples are 7.23–8.15%. The average values of V_{daf} from the II ore body are 3.93%, and the V_{daf} values of the samples from No. the I ore body are around 5.0%. The d_{002} value of the II ore body is 0.3433–0.3389 nm, with an average of 0.3410 nm; the G value of the II ore body is 8.14–59.30%, with an average of 35.19%. Combining previous R_{\max} and V_{daf} data, it can be determined that the samples of the II ore body are coal-hosted graphite. The d_{002} value of the I ore body is 0.3418–0.3429 nm, with an outlier of 0.3622 nm; the G value of the II ore body is 12.79–25.58%, with an average of 18.22%. Combining previous R_{\max} and V_{daf} data, it can be determined that some samples of the I ore body are coal-hosted graphite, and some samples are coal.
- (2) The coupling effect of magmatic thermodynamics and tectonic stress jointly controlled the enrichment of coal-hosted graphite deposits in Feng County, west Qinling orogenic belt. Magmatic thermal emplacement provided sufficient thermodynamic conditions for coal seam heating to form graphite. Especially during the Yanshan period, the strong magmatic thermal process provided important thermodynamic factors for coal graphitization. Additionally, regional metamorphism plays an active role in graphite deposit enrichment.
- (3) The nearly north–south compressive structures in the study area were formed during the Indosinian period and activated and strengthened during the Yanshan period, overlapping with the nearly east–west compression structure during the Himalayan period, which provided effective tectonic stress for the evolution of coal graphitization. Tectonic stress catalyzed the graphitization process; the stacking effect of BSUs is the microscopic mechanism of coal graphitization. Under tectonic stress, the basic structural units (BSUs) rotated and rearranged, eventually forming a straight graphite structure. The tectonic stress also controlled the spatial distribution of graphite deposits. The core of the secondary anticlines and synclines of the complex fold system is rich in banded enriched graphite deposits.

Author Contributions: Conceptualization, Y.F. and L.L.; methodology, Y.F. and Y.R.; software, Y.R.; validation, L.L.; formal analysis, Y.R. and L.L.; investigation, Y.F. and L.L.; resources, Y.F. and L.L.; data curation, Y.F. and Y.R.; writing—original draft preparation, Y.F.; writing—review and editing, Y.F. and Y.R.; visualization, Y.R. and L.L.; supervision, L.L.; project administration, Y.F. All authors have read and agreed to the published version of the manuscript.

Funding: This research was supported by Key R&D and promotion projects in Henan Province (No. 232102320319), Jiangxi Provincial Natural Science Foundation (No. 20202BABL211019), Natural Science Foundation of China (No. 41502081), Cultivation Fund of National Natural Science Foundation of Nanyang Normal University (No. 2022PY009), and Doctoral program of Nanyang Normal University (No. 2022ZX040), China’s Ministry of Education University-Industry Cooperative Education Program (No. 220902284303850), Henan Province Undergraduate Innovation and Entrepreneurship Training Program (No. 202310481032), Teaching and research projects of Nanyang Normal University (No. 2023-JXYJYB-11, No. 2023ZLGC07).

Data Availability Statement: Not applicable.

Acknowledgments: Special thanks are given to Senior Engineer Guangchao Zhang, Yunxun Wei, Zhuo Liu, Long Yu, Yitong Su for their selfless assistance in the field investigations. Thanks to the editor and reviewers for their detailed and constructive comments on this manuscript.

Conflicts of Interest: The authors declare no conflict of interest.

References

1. Sun, S.L.; Wu, G.Q.; Cao, D.Y.; Ning, S.Z.; Qiao, J.W.; Zhu, H.X.; Zhu, S.F.; Miao, Q. Mineral Resources in Coal Measures and Development Trend. *Coal Geol. China* **2014**, *26*, 1–11, (In Chinese with English abstract). [[CrossRef](#)]

2. Cao, D.Y.; Zhang, H.; Dong, Y.J.; Wu, G.Q.; Ning, S.Z.; Mo, J.F.; Li, X. Research status and key orientation of coal-based graphite mineral geology. *Earth Sci. Front.* **2017**, *24*, 317–327. (In Chinese with English abstract). [[CrossRef](#)]
3. Cao, D.Y.; Wang, L.; Zhu, W.Q.; Wu, G.Q.; Wei, Y.C.; Ning, S.Z.; Wang, G.X.; Xiao, J.C.; Xu, X.; Liu, K. Discussion on identification standard of coal-measure graphite. *Coal Geol. Explor.* **2022**, *50*, 105–113. (In Chinese with English abstract). [[CrossRef](#)]
4. Wang, D.L.; Ren, H.; Zhang, Y.H.; Wang, G.X.; Zheng, H.Y.; Wang, K.L.; Wen, M. Probe into coal measures graphite resources exploitation and utilization status quo in China and countermeasures proposal. *Coal Geol. China* **2022**, *34*, 8–10. (In Chinese with English abstract) [[CrossRef](#)]
5. Yan, L.Y.; Gao, S.X.; Chen, Z.G.; Jiao, L.X.; Sun, L.; Liu, Y.F.; Zhou, W. Metallogenic characteristics and metallogenic zoning of graphite deposits in China. *Geol. China* **2018**, *45*, 421–440. (In Chinese with English abstract) [[CrossRef](#)]
6. Ponnusamy, M.; Ramya, K.C.; Sivasankaran, V.; Farmani, H.; Farmani, A. Correction to: Emerging advanced photonics applications of graphene and beyond-graphene 2D materials: Recent advances. *J. Mater. Res.* **2022**, *37*, 1133. [[CrossRef](#)]
7. Yang, K.; Feng, L.Z.; Hong, H.; Cai, W.B.; Liu, Z. Preparation and functionalization of graphene nanocomposites for biomedical applications. *Nat. Protoc.* **2013**, *8*, 2392–2403. [[CrossRef](#)]
8. U.S. Geological Survey (USGS). *Mineral Commodity Summaries*; USGS: Reston, VA, USA, 2023; p. 82.
9. Zhang, S.J.; Wang, N.; Cui, L.W.; Ji, G.Y.; Deng, W.B.; Zhang, Y.W. Analysis of supply and demand situation of graphite resources at home and abroad. *Inorg. Chem. Ind.* **2021**, *53*, 1–11. [[CrossRef](#)]
10. Weber, L. On the security of graphite supply. *Mineral. Petrol.* **2023**, *117*, 387–399. [[CrossRef](#)]
11. Sun, L.; Xu, C.P.; Xiao, K.Y.; Zhu, Y.S.; Yan, L.Y. Geological characteristics, metallogenic regularities and the exploration of graphite deposits in China. *China Geol.* **2018**, *1*, 425–434. [[CrossRef](#)]
12. Mo, R.J.; Liu, S.B.; Huang, C.R. *Geology of Graphite Deposits in China*; China Architecture & Building Press: Beijing, China, 1989. (In Chinese)
13. Feng, Y.W.; Qu, H.J.; Lv, L.S. Distribution Characteristics and metallogenic Regularity of Graphite Deposits in Qinling Orogen, China. *Acta Geol. Sin. (Engl. Ed.)* **2015**, *89*, 1244–1263. [[CrossRef](#)]
14. Cao, D.Y.; Wei, Y.C.; Li, Y.; Liu, Z.F.; Li, H.T.; Wang, L.; Wu, G.Q.; Ning, S.Z.; Xu, X. Determination of identification index and construction of classification and classification system of coal measures graphite. *J. China Coal Soc.* **2021**, *46*, 1833–1846. (In Chinese with English abstract) [[CrossRef](#)]
15. Wang, L.; Fan, J.L.; Feng, Y.W. Graphite Resources Status Quo and Distribution of Graphite Deposits in China. *Coal Geol. China* **2017**, *29*, 5–9. (In Chinese with English abstract) [[CrossRef](#)]
16. Feng, Y.W.; Lyu, L.S. Analysis of geological characteristics and genesis of Carboniferous coal-based graphite deposit in Feng County, Shaanxi Province. *China Coal* **2018**, *44*, 44–48. (In Chinese with English abstract)
17. Cao, D.Y.; Zhan, W.F.; Li, X.M. Effect of Intrusion of the Shangcheng Granite Body on Structural Framework of the Yangshan Coal-Bearing Series, the Beihuaiyang Area, China. *J. China Univ. Min. Technol.* **2007**, *36*, 320–324. (In Chinese with English abstract) [[CrossRef](#)]
18. Peng, J.C. Formation Mechanism of High Metamorphism Coal Belt in The Southern Margin of The North China Plate. Ph.D. Thesis, China University of Mining and Technology, Beijing, China, 2015; pp. 1–136. (In Chinese with English abstract)
19. Teichmüller, M.; Teichmüller, R. Geological causes of coalification. *Coal Sci. Am. Adv. Chem. Ser.* **1966**, *55*, 133–155. [[CrossRef](#)]
20. Yang, Q.; Ren, D.Y. Discussion on the issue of coal metamorphism in China. *Coal Geol. Explor.* **1981**, *9*, 1–10. (In Chinese with English abstract)
21. Hower, J.C.; Fiene, F.L.; Wild, G.D.; Helfrich, C.T. Coal metamorphism in the upper portion of the Pennsylvanian sturgis formation in western Kentucky. *Geol. Soc. Am.* **1983**, *94*, 1475–1481. [[CrossRef](#)]
22. McFarlane, C.G. Igneous metamorphism of coal beds. *Econ. Geol.* **1929**, *24*, 10. [[CrossRef](#)]
23. Harrison, M.J.; Marshak, S.; Onasch, C.M. Stratigraphic control of hot fluids on anthracitization, Lackawanna synclinorium, Pennsylvania. *Tectonophysics* **2004**, *378*, 85–103. [[CrossRef](#)]
24. Fowler, P.; Gayer, R.A. The association between tectonic deformation, inorganic composition and coal rank in the bituminous coals from the South Wales Coalfield, United Kingdom. *Int. J. Coal Geol.* **1999**, *42*, 1–31. [[CrossRef](#)]
25. Suchy, V.; Frey, M.; Wolf, M. Vitrinite reflectance and shear-induced graphitization in orogenic belts: A case study from the Kandersteg area, Helvetic Alps, Switzerland. *Int. J. Coal Geol.* **1997**, *34*, 1–20. [[CrossRef](#)]
26. Wang, L.; Cao, D.; Peng, Y.; Ding, Z.; Li, Y. Strain-Induced Graphitization Mechanism of Coal-Based Graphite from Lutang, Hunan Province, China. *Minerals* **2019**, *9*, 617. [[CrossRef](#)]
27. Wu, Y.Q.; Zhang, Q.; Shao, G.L.; Jiao, S.T.; Xu, Y.H.; Yang, Y.L. Yang's Coal Metamorphism Theory—A Valuable Result of Chinese Coal Geological Theory and Practices. *Coal Geol. China* **2016**, *28*, 1–7. [[CrossRef](#)]
28. Ao, T.; Kalita, P.; Blada, C.; Brown, N.P.; Fulford, K.; Gard, P.; Geissel, M.; Hanshaw, H.; Montoya, M.; Payne, S.; et al. Exploring the High-Pressure Phases of Carbon through X-ray Diffraction of Dynamic Compression Experiments on Sandia's Z Pulsed Power Facility. *Minerals* **2023**, *13*, 1203. [[CrossRef](#)]
29. Bustin, R.M.; Rouzaud, J.N.; Ross, J.V. Natural graphitization of anthracite: Experimental considerations. *Carbon* **1995**, *33*, 679–691. [[CrossRef](#)]
30. Rodrigues, S.; Marques, M.; Suárez-Ruiz, I.; Camean, I.; Flores, D.; Kwiecinska, B. Microstructural investigations of natural and synthetic graphites and semi-graphites. *Int. J. Coal Geol.* **2013**, *111*, 67–79. [[CrossRef](#)]

31. Cao, D.Y.; Wang, L.; Ding, Z.Y.; Peng, Y.W.; Li, Y. Characterization of the Heterogeneous Evolution of the Nanostructure of Coal-Based Graphite. *J. Nanosci. Nanotechnol.* **2021**, *21*, 670–681. [[CrossRef](#)]
32. Li, K.; Zhang, H.; Wu, Y.T.; Hu, M.S.; Liu, Q.F. Graphite microcrystals growth in naturally graphitized coal from Hunan, China. *J. Cryst. Growth* **2022**, *582*, 126530. [[CrossRef](#)]
33. Li, K.; Rimmer, S.M.; Liu, Q.F. Geochemical and petrographic analysis of graphitized coals from central Hunan, China. *Int. J. Coal Geol.* **2018**, *195*, 267–279. [[CrossRef](#)]
34. Sun, M.S. *Instructions for the 1/50000 Regional Geological Map of Honghuapu I48E012020*; Regional Survey Institute of Shaanxi Geological Survey Bureau: Xi'an, China, 1995; pp. 1–63. (In Chinese)
35. Zhang, Y.F.; Yang, T.; Yi, P.F.; Liu, X.D.; He, Y.F.; Yao, Z.; Wu, T.; Ma, X.Q. Shaanxi Institute of Geological Survey: 1/50000 Geological Map Dataset of Xinjiazhuang (I48E012019) at the border between Shaanxi Province and Gansu Province. *Geol. Sci. Data Publ. Syst.* **2022**. [[CrossRef](#)]
36. Zhang, G.C.; Bao, Z.H.; Li, C.C. *General Survey Report on Graphite Mines in the Peripheral Area of Yanwan Mining Area, Feng County, Shaanxi Province*; Aerial Photogrammetry and Remote Sensing Group Co., Ltd. of CNACG (ARSC): Ningbo, China, 2017.
37. Wei, Y.X.; Lv, L.S.; Li, C.C. Structural characteristics and prospecting direction of coal-based graphite deposits in Feng county area, China. *IOP Conf. Ser. Earth Environ. Sci.* **2020**, *558*, 022041. [[CrossRef](#)]
38. Feng, Y.W.; Lv, L.S. Analysis on the Genesis of Carboniferous Cryptocrystalline Graphite Deposits in the Western Qinling Mountains. In Proceedings of the 8th National Symposium on Metallogenic Theory and Prospecting Methods, Nanchang, China, 9–12 December 2017; pp. 77–78. (In Chinese with English abstract)
39. Zhang, G.W.; Guo, A.L.; Dong, Y.P.; Yao, A.P. Rethinking of the Qinling orogen. *J. Geomech.* **2019**, *25*, 746–768. [[CrossRef](#)]
40. Zhang, G.W.; Men, Q.R.; Yu, Z.P.; Sun, Y.; Zhou, D.W.; Guo, A.L. Orogenesis and dynamics of the Qinling Orogen. *Sci. China Ser. D* **1996**, *39*, 225–234.
41. Dong, Y.P.; Liu, X.M.; Zhang, G.W.; Chen, Q.; Zhang, X.N.; Li, W.; Yang, C. Triassic diorites and granitoids in the Foping area: Constraints on the conversion from subduction to collision in the Qinling orogen, China. *J. Asian Earth Sci.* **2012**, *47*, 123–142. [[CrossRef](#)]
42. Guo, P.Y.; Niu, Y.L.; Yu, X.H. A synthesis and new perspective on the petrogenesis of kamafugites from West Qinling, China, in a global context. *J. Asian Earth Sci.* **2014**, *79*, 86–96. [[CrossRef](#)]
43. *GB/T3519-2008*; Amorphous Graphite. The Standardization Administration of the People's Republic of China: Beijing, China, 2008.
44. Buseck, P.R.; Beyssac, O. From Organic Matter to Graphite: Graphitization. *Elements* **2014**, *10*, 421–426. [[CrossRef](#)]
45. Kwiecieńska, B.; Petersen, H.I. Graphite, semi-graphite, natural coke, and natural char classification-ICCP system. *Int. J. Coal Geol.* **2004**, *57*, 99–116. [[CrossRef](#)]
46. Rantitsch, G.; Lämmerer, W.; Fisslthaler, E.; Mitsche, S.; Kaltenböck, H. On the discrimination of semi-graphite and graphite by Raman spectroscopy. *Int. J. Coal Geol.* **2016**, *159*, 48–56. [[CrossRef](#)]
47. Lan, C.Y.; Tang, Y.G.; Huan, X.; Che, Q.L. Effects of Minerals in Anthracite on the Formation of Coal-Based Graphene. *Chem. Sel.* **2019**, *4*, 5937–5944. [[CrossRef](#)]
48. Li, H.T.; Cao, D.Y.; Zou, X.Y.; Zhu, Z.R.; Zhang, W.G.; Xia, Y. Raman spectroscopic characterization and surface graphitization degree of coal-based graphite with the number of aromatic layers. *Spectrosc. Spectr. Anal.* **2022**, *42*, 2616–2623. [[CrossRef](#)]
49. Wang, Y.H.; Yao, S.P. Effect of pressure on the evolution of vitrinite graphitized mesophases: An experimental study on anthracite under high temperature and pressure. *Int. J. Coal Geol.* **2023**, *267*, 104187. [[CrossRef](#)]
50. Kostova, I.; Tormo, L.; Crespo-Feo, E.; Garcia-Guinea, J. Study of coal and graphite specimens by means of Raman and cathodoluminescence. *Spectrochim. Acta Part A Mol. Biomol. Spectrosc.* **2012**, *91*, 67–74. [[CrossRef](#)] [[PubMed](#)]
51. Guo, Q.; Mao, X.H.; Zhang, J.X.; Wu, Y.W. Paleozoic tectonothermal evolution in the west Qinling orogen, central China: Petrological and chronological evidence from garnet amphibolites. *Minerals* **2023**, *13*, 1183. [[CrossRef](#)]
52. Mercier, J.L.; Vergely, P.; Zhang, Y.Q.; Hou, M.J.; Bellier, O.; Wang, Y.M. Structural records of the Late Cretaceous-Cenozoic extension in Eastern China and the kinematics of the Southern Tan-Lu and Qinling Fault Zone (Anhui and Shaanxi provinces, PR China). *Tectonophysics* **2013**, *582*, 50–75. [[CrossRef](#)]

Disclaimer/Publisher's Note: The statements, opinions and data contained in all publications are solely those of the individual author(s) and contributor(s) and not of MDPI and/or the editor(s). MDPI and/or the editor(s) disclaim responsibility for any injury to people or property resulting from any ideas, methods, instructions or products referred to in the content.